



Transition metal complexes with thiosemicarbazide-based ligands. Part 60. Reactions of copper(II) bromide with pyridoxal S-methylthiosemicarbazone (PLITSC). Crystal structure of $[\text{Cu}(\text{PLITSC}-\text{H})\text{H}_2\text{O}]\text{Br}\cdot\text{H}_2\text{O}$

VUKADIN M. LEOVAC^{1*}, LJILJANA S. VOJINOVIĆ-JEŠIĆ^{1#}, SONJA A. IVKOVIĆ^{2#},
MARKO V. RODIĆ^{1#}, LJILJANA S. JOVANOVIĆ^{1#}, BERTA HOLLÓ^{1#}
and KATALIN MÉSZÁROS SZÉCSÉNYI^{1#}

¹Faculty of Sciences, University of Novi Sad, Trg D. Obradovića 3, 21000 Novi Sad, Serbia

and ²Faculty of Environmental Protection, University EDUCONS, V. Putnika bb, 21208
Sremska Kamenica, Serbia

(Received 22 June, revised 20 August 2013)

Abstract: The synthesis and structural characterization of a square-planar copper(II) complex with pyridoxal S-methylthiosemicarbazone (PLITSC) of the formula $[\text{Cu}(\text{PLITSC}-\text{H})\text{H}_2\text{O}]\text{Br}\cdot\text{H}_2\text{O}$ (**1**) as the first Cu(II) complex with a monoanionic form of this ligand were described. Complex **1** together with two previously synthesized complexes $[\text{Cu}(\text{PLITSC})\text{Br}_2]$ (**2**) and $[\text{Cu}(\text{PLITSC})\text{Br}(\text{MeOH})]\text{Br}$ (**3**) were characterized by elemental analysis, IR and electronic spectroscopy and by the methods of thermal analysis, conductometry and magnetochemistry.

Keywords: copper(II) complexes; pyridoxal S-methylthiosemicarbazone; crystal structure; spectra; thermal analysis.

INTRODUCTION

Metal complexes with Schiff base derivatives of pyridoxal, which is one of the six natural forms of vitamin B6, due to their interesting chemical, structural and biological characteristics, have been the subject of many studies.¹ A special group of Schiff base derivatives of pyridoxal consists of its compounds with semi-, thiosemi- and isothiosemicarbazones, which were found to coordinate as ONO, ONS and ONN ligands, respectively.² The coordination chemistry of pyridoxal thiosemicarbazone (PLTSC) began in 1986 with the papers of Ferrari Belicchi *et al.*³ and since then, this ligand has been used for the syntheses of many complexes, not only with transition, but also with some non-transition

* Corresponding author. E-mail: vukadin.leovac@dh.uns.ac.rs

Serbian Chemical Society member.

doi: 10.2298/JSC130622084L

metals.^{2–8} In contrast to this ligand, the coordination chemistry of the *S*-methyl derivative, *i.e.*, pyridoxal *S*-methylisothiosemicarbazone (PLITSC) commenced later with the papers of Leovac *et al.*,^{2,9,10} which is the reason for the smaller number of described complexes [Cu(II),² Fe(III),^{2,9,10} Co(III),^{2,11} Ni(II),¹² V(V) and Mo(VI)¹³]. It was found that this tridentate ONN ligand can be coordinated as neutral, mono- and di-anionic species, which was proven by, among other methods, X-ray structural analysis of its complexes.^{2,11–15} The structures of two square-pyramidal Cu(II) complexes with the neutral ligand, [Cu(PLITSC)-NO₃(H₂O)]NO₃¹⁴ and [Cu(PLITSC)Br(MeOH)]Br,¹⁵ and one square-planar complex with its di-anionic form [Cu(PLITSC-2H)NH₃]·H₂O·0.5 MeOH² have been already determined. In this paper, we describe the synthesis and structure of the first Cu(II) complex with a monoanionic PLITSC ligand [Cu(PLITSC-H)-H₂O]Br·H₂O (**1**) and its IR and UV–Vis spectral, thermal and some other physical characteristics are described. The same data are given for the previously synthesized copper(II) bromide complexes of PLITSC [Cu(PLITSC)Br₂] (**2**) and [Cu(PLITSC)Br(MeOH)]Br (**3**) and compared with the corresponding data of the newly synthesized compound **1**.

EXPERIMENTAL

Reagents

All employed chemicals were commercial products of analytical reagent grade, except for the ligand pyridoxal *S*-methylisothiosemicarbazone, which was prepared by the reaction of EtOH solutions of pyridoxal hydrochloride and *S*-methylisothiosemicarbazide hydroiodide, and subsequent neutralization with an aqueous solution of Na₂CO₃.¹⁴

Synthesis of the complexes

[Cu(PLITSC-H)H₂O]Br·H₂O (**1**). A mixture of PLITSC (0.075 g, 0.25 mmol) and CuBr₂ (0.065 g, 0.3 mmol) was dissolved in a mixture of 8 cm³ EtOH and 2 cm³ H₂O with mild heating. After 4 days at room temperature, the brown single crystals, obtained from the brown–green solution were filtered off and washed with EtOH. Yield: 0.030 g.

The other two complexes were prepared according to procedures described in the literature,^{15,16} *i.e.*, by the reactions of CuBr₂ and the ligand in ethanol (**2**) or methanol (**3**).

Analytical methods

Elemental analyses (C, H, N, S) of air-dried complexes were realized by standard micro-methods.

The molar conductivities of freshly prepared EtOH and MeOH solutions of the complexes ($c = 1 \times 10^{-3}$ mol dm⁻³) were measured on a Jenway 4010 conductivity meter.

The magnetic susceptibility measurements were conducted at room temperature on an MSB-MK1 magnetic susceptibility balance, Sherwood Scientific Ltd., Cambridge, UK.

The IR spectra were recorded as KBr pellets on a Thermo Nicolet NEXUS 670 FT-IR spectrophotometer in the range of 4000–400 cm⁻¹.

The electronic spectra of the complexes in DMF and MeOH solutions were recorded on a T80+ UV/Vis spectrometer PG Instruments Ltd. in the spectral range 270–1100 nm (DMF) and 210–1100 nm (MeOH).

Thermal data were obtained using a TA Instruments SDT-Q600 TGA/DSC instrument at 20 °C min⁻¹ heating rate under a dynamic N₂ atmosphere (flow rate of 100 cm³ min⁻¹) in alumina crucibles and with sample masses of ≈2 mg.

Single crystal X-ray crystallography

A single crystal of **1** was selected, glued on glass fiber and mounted on a Gemini S κ-geometry diffractometer (Agilent Technologies). A sealed tube with a Cu-anode was used as X-radiation source, which was monochromatized with a graphite crystal (CuKα, λ = 1.5418 Å). The diffraction pattern, obtained in the ω scan mode, was recorded with a Sapphire3 CCD area detector. Data collection, reduction, absorption correction (numerical, based on Gaussian integration over a multifaceted crystal model) and cell refinement were performed with CRYSTALISPRO.¹⁷ The structure was solved by a direct method using Sir92¹⁸ and refined on F² with the SHELXL-2013 program¹⁹ integrated in SHELXL²⁰ graphical user interface. Carbon bonded hydrogen atoms were introduced in idealized positions (CH, CH₂) and refined as riding with U_{iso} fixed as 1.2U_{eq} of the parent atoms, while in the case of CH₃ groups, the torsion angle was refined and U_{iso} was fixed as 1.5U_{eq} of the parent atoms. Positions of hydrogen atoms bonded to heteroatoms were taken from ΔF map and refined as riding, while their U_{iso} were refined, except for H4A where U_{iso} was fixed as 1.2 U_{eq} of the N4. A summary of the crystallographic data is given in Table I. Structural data were validated and analyzed with PLATON.²¹ Figures were produced using ORTEP-3 and PLATON.²²

TABLE I. Crystallographic data for [Cu(H₂O)(PLITSC–H)]Br·H₂O (**1**)

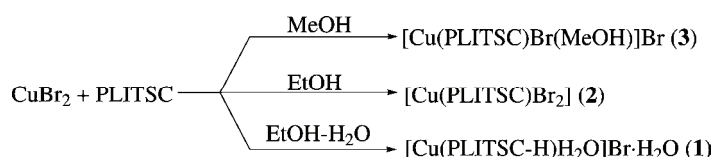
Crystal data		Data collection and refinement	
Molecular formula	C ₁₀ H ₁₇ BrCuN ₄ O ₄ S	Temperature, K	298(2)
Formula weight	432.79	Wavelength, Å	1.5418
Crystal system	Orthorhombic	θ range, °	3.6–72.2
Space group	Pna2 ₁	No. reflcns. measd.	3205
a / Å	6.9360 (3)	No. unique reflcns.	2010
b / Å	24.535 (1)	R _{int}	0.021
c / Å	8.9512 (4)	No. reflcns. with I > 2σI	1838
V / Å ³	1523.3 (1)	No. restraints	1
Z	4	No. refined parameters	199
D _c / g cm ⁻³	1.887	Goodness-of-fit on F ²	1.05
μ (CuKα) / mm ⁻¹	6.58	R and wR (I > 2σI)	0.030 and 0.074
F(000)	868	R and wR (all data)	0.035 and 0.078
Crystal size, mm	0.40 × 0.20 × 0.03	Δρ _{max} and Δρ _{min} , e Å ⁻³	0.40 and –0.33
Color / shape	Brown / plate		

RESULTS AND DISCUSSION

Synthesis and some physicochemical characteristics of the complexes

The newly synthesized complex Cu(PLITSC–H)H₂O]Br·H₂O (**1**) was obtained in the reaction of CuBr₂ and PLITSC (mole ratio 1:1) in warm 80 % ethanol. As can be seen from the formula, PLITSC is coordinated in its mono-anionic form, which is obtained after deprotonation of the thioureido moiety. Since it was shown^{15,16} that in the reaction of the same reactants but in the pure solvents (EtOH and MeOH), complexes **2** and **3** were formed containing the

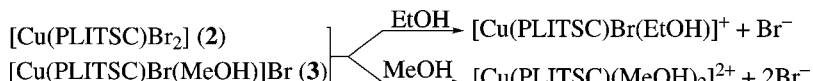
neutral ligand form (Scheme 1), it could be concluded that the nature of the solvent has a striking influence on the form of the coordinated PLITSC. Namely, since the N–H bond weakens on coordination of the terminal nitrogen atom, the presence of water as a better proton acceptor than alcohol causes deprotonation of the ligand and the formation of **1**.



Scheme 1. Reactions of the syntheses of the complexes.

The type of the ligand deprotonation has a significant impact on the geometry of the complexes. Namely, the newly synthesized **1** with monodeprotonated PLITSC has a square-planar structure (*vide infra*). In contrast, in complex **3**, the square-pyramidal structure¹⁵ is realized by a tridentate ONN coordination of the neutral PLITSC, one methanol molecule and one bromide ion. The change in the coordination geometry is a result of the increasing ligand field strength of PLITSC, caused by the deprotonation of the thioureido moiety, *i.e.* the increase in the donor ability of the coordinated terminal nitrogen atom. The structure of the desolvato complex **2** is most probably square pyramidal, realized by the tridentate coordination of PLITSC and the coordination of two bromido ligands. The value of the molar conductivity of ethanolic solution of **2** ($\Lambda_M = 39 \text{ S cm}^2 \text{ mol}^{-1}$) is characteristic for 1:1 electrolytes,²³ which refers to the coordination of only one bromide in solution with presumably $[\text{Cu}(\text{PLITSC})\text{Br}(\text{EtOH})]^+$ the most dominant species (Scheme 2). An almost identical value of Λ_M was found in an ethanolic solution of the similar $[\text{Cu}(\text{PLSC})\text{Br}_2]$ complex with the ONO tridentate pyridoxal semicarbazone (PLSC) ligand ($\Lambda_M = 38 \text{ S cm}^2 \text{ mol}^{-1}$). As it was shown by X-ray structure analysis that in $[\text{Cu}(\text{PLSC})\text{Br}_2]$, beside tridentate PLSC coordination, both bromides acted as co-ligands,²⁴ it might be supposed that two bromide ions are also coordinated in the crystals of complex **2**. Hence, it is reasonable to ascribe a penta-coordinated structure for complex **2**. It is noteworthy that $[\text{Cu}(\text{PLITSC})(\text{H}_2\text{O})\text{NO}_3]\text{NO}_3$ also has a square-pyramidal structure.¹⁴ In contrast to the molar conductivity of an ethanolic solution of **2**, referring to a 1:1 electrolyte, the value of the molar conductivity of its methanolic solution ($\Lambda_M = 141 \text{ S cm}^2 \text{ mol}^{-1}$) corresponds to 2:1 electrolytes.²³ This means that due to stronger solvolysis effects of MeOH compared to EtOH, in methanolic solutions both bromido-ligands are replaced with two solvent molecules. The same holds for **3**, *i.e.*, the molar conductivity of its MeOH solution ($\Lambda_M = 164 \text{ S cm}^2 \text{ mol}^{-1}$) refers to the replacement of the coordinated bromide. This was not the case with its EtOH solution with a significantly lower

molar conductivity ($\Lambda_M = 36 \text{ S cm}^2 \text{ mol}^{-1}$). Hence, it could be concluded that **2** and **3** in the solutions of the cited alcohols behave in the same manner (Scheme 2). The molar conductivity of methanolic solution of **1** is in accordance with its coordination formula ($\Lambda_M = 73 \text{ S cm}^2 \text{ mol}^{-1}$).



Scheme 2. Solvolysis reactions of complexes **2** and **3** in alcoholic solutions.

All three complexes are paramagnetic and the values of their effective magnetic moments are 1.78, 1.86 and 1.84 μ_B for **1**, **2** and **3**, respectively. The values are in the usual range for magnetically dilute Cu(II) compounds and only negligible spin–spin coupling, characteristic of dinuclear structures²⁵ might be present.

With the exception of **3**, which loses methanol, the other two complexes are stable at room temperature. All the complexes are well soluble in DMF, less soluble in MeOH and EtOH and insoluble in Et_2O .

Analytic and spectral data

[Cu(PLITSC-H) $H_2\text{O}$]Br· $H_2\text{O}$ (1). Anal. Calcd. for $\text{CuC}_{10}\text{H}_{17}\text{BrN}_4\text{O}_4\text{S}$ (FW: 432.79): C, 27.73; H, 3.93; N, 12.94; S, 7.41 %. Found: C, 27.48; H, 3.90; N, 12.88; S, 7.49 %. IR (KBr, cm^{-1}): 3311, 3217, 2940, 2817, 1566, 1493, 1375, 1326, 1241, 1325, 1153, 1011, 905, 843, 718, 650; UV–Vis (DMF, λ / nm ($\log (\varepsilon / \text{M}^{-1} \text{ cm}^{-1})$)): 320 (3.88), 366 (3.88), 390 (3.97), 424 (4.18), 444 (4.25), (MeOH, λ / nm ($\log (\varepsilon / \text{M}^{-1} \text{ cm}^{-1})$)): 243 (4.20), 265sh (4.18), 318 (3.74), 362sh (3.81), 380 (3.94), 413sh (415), 430 (4.23); molar conductivity (MeOH, $\Lambda_M / \text{S cm}^2 \text{ mol}^{-1}$): 73; magnetic moment (μ_{eff} / μ_B): 1.78.

[Cu(PLITSC)Br₂] (2). Anal. Calcd. for $\text{CuC}_{10}\text{H}_{14}\text{Br}_2\text{N}_4\text{O}_2\text{S}$ (FW: 477.65): C, 25.14; H, 2.95; N, 11.73; S, 6.71 %. Found: C, 25.56; H, 3.02; N, 11.78; S, 6.39 %. IR (KBr, cm^{-1}): 3291, 3093, 2958, 2884, 2754, 1562, 1429, 1381, 1291, 1244, 1146, 1008, 907, 856, 782, 615. UV–Vis (DMF, λ / nm ($\log (\varepsilon / \text{M}^{-1} \text{ cm}^{-1})$)): 298 (4.00), 323 (3.97), 390sh (3.95), 414 (4.00), 442 (3.92), 642sh (2.15), (MeOH, λ / nm ($\log (\varepsilon / \text{M}^{-1} \text{ cm}^{-1})$)): 244 (4.30), 282 (3.90), 320 (3.91), 333sh (3.84), 388sh (3.95), 401 (3.99), 655 (1.90); molar conductivity (MeOH, $\Lambda_M / \text{S cm}^2 \text{ mol}^{-1}$): 141 (EtOH, $\Lambda_M / \text{S cm}^2 \text{ mol}^{-1}$): 39; magnetic moment (μ_{eff} / μ_B): 1.86.

[Cu(PLITSC)Br(MeOH)]Br (3). Anal. Calcd. for $\text{CuC}_{11}\text{H}_{18}\text{Br}_2\text{N}_4\text{O}_3\text{S}$ (FW: 509.70): C, 25.92; H, 3.56; N, 10.99; S, 6.29 %. Found: C, 25.86; H, 3.42; N, 10.78; S, 6.16 %. IR (KBr, cm^{-1}): 3323, 3239, 3112, 2945, 2816, 2718, 1566, 1546, 1437, 1387, 1326, 1307, 1242, 1158, 1036, 1000, 911, 853, 753, 576. UV–Vis (DMF, λ / nm ($\log (\varepsilon / \text{M}^{-1} \text{ cm}^{-1})$)): 298 (4.00), 325 (3.97), 392sh (3.94), 413 (3.99), 442 (3.83), 642sh (2.19), (MeOH, λ / nm ($\log (\varepsilon / \text{M}^{-1} \text{ cm}^{-1})$)): 244

(4.34), 285 (3.94), 320 (3.95), 334sh (3.88), 388sh (3.99), 401 (4.00), 655 (2.00); molar conductivity, (MeOH, Λ_M / S cm² mol⁻¹): 164, (EtOH, Λ_M / S cm² mol⁻¹): 36; magnetic moment (μ_{eff} / μ_B): 1.84.

IR and electronic spectra

In IR spectra, $\nu(\text{OH})$ bands (H₂O, -CH₂OH, CH₃OH) and $\nu(\text{NH})$ bands are observed at 3311 and 3217 (**1**), 3291 and 3093 (**2**) and 3323, 3239 and 3112 cm⁻¹ (**3**). The well-defined $\nu(\text{NH}^+)$ band of the vibrations of the protonated pyridine nitrogen in the spectra of **1** and **2** are at 2817 and 2754 cm⁻¹,^{2,4} respectively, contrary to **3**, which in this range has one broad and unresolved band. The $\nu(\text{C}=\text{N})$ band for all three complexes is located at \approx 1565 cm⁻¹ and in comparison to the same band of the free ligand (1655 cm⁻¹) is shifted to lower energy due to coordination of the azomethine nitrogen.^{26,27} In contrast to this, as a result of the coordination of oxygen, a positive energy shift for the deprotonated phenolic hydroxyl, $\nu(\text{C}-\text{O})$, was observed. In the spectrum of the ligand, the band is at 1255 cm⁻¹ while it appears at 1326, 1291 and 1307 cm⁻¹ in the spectra of the complexes **1**, **2** and **3**, respectively.^{28,29}

In the available electronic spectral range, the spectra of the complexes display multiple, mainly unresolved bands of all kinds. Generally, the spectra of the complexes **2** and **3** are similar but different from those of **1**. The similarity of the spectra for **2** and **3** could be another proof of their similar structure.

In all the complexes, the strong band at the blue end of the spectra in MeOH (at about 244 nm) can be ascribed to $\pi \rightarrow \pi^*$ pyridine ring absorptions which are, due to conjugation in the complexes, shifted by 25 nm to higher wavelengths compared to those of the ligand alone.^{9,30} Other bands in the intraligand absorption region ($\lambda < 360$ nm) are poorly developed particularly in DMF due to partial overlapping of $\pi \rightarrow \pi^*$ imine and $n \rightarrow \pi^*$ of both imine and pyridine ring, which are also present in the spectra of the ligand.

All the complexes have very strong absorptions at about 400–450 nm, which belong to charge transfers and show complex solvation effects. The striking similarity of the spectra for **2** and **3** in each solvent, which is particularly obvious in this range, is a consequence of replacement of coordinated Br and MeOH by solvent molecules, thus forming the same complex structure (*vide infra*).

Additional characteristics of the CT bands at their long-wave sides is their complete overlapping with d-d transitions in the spectra for **1**, or partial merging for the other complexes, which therefore are seen as shoulders. In addition, very weak absorptions at wavelengths 850–900 nm cannot be precisely determined due to their overlapping with long-wave sides of comparatively stronger d-d bands. The recorded d-d transitions have negative solvatochromic effect because of better stabilization by solvation of the ground state molecule.

Crystal structure of **1**

The molecular structure of the complex is shown in Fig. 1, whilst selected bond distances and angles are given in Table II. The asymmetric unit contains the complex cation, one water molecule and one bromide anion. The copper atom is situated in a square-planar environment made by ONN tridentate coordination of the organic ligand and one water molecule. Metal–ligand bond lengths are in the expected range (1.898 (4)–1.948 (5) Å), the M–O1 (phenoxide oxygen) being the shortest one and that of M–O3 (water oxygen) the longest one. The different metal–chelate ligand bond lengths are consistent with the electronic structure of PLITSC–H. Namely, due to the located negative charge, the phenoxide oxygen atom is the best electron donor, and as such builds the shortest bond. Due to ligand deprotonation (*vide infra*), the electron density is increased on the N1–C1–N2 fragment and is probably responsible for the slightly shorter Cu–N1 compared to the Cu–N3 bond.

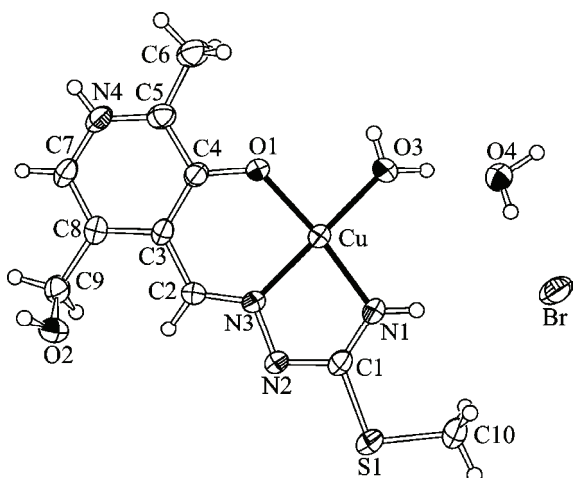


Fig. 1. Molecular structure of [Cu(PLITSC–H)(H₂O)]Br·H₂O (**1**).

TABLE II. Selected bond lengths and valence angles for **1**

Bond	Distance, Å	Bonds	Angle, °
Cu–O1	1.898 (4)	N1–Cu–N3	81.3 (2)
Cu–N1	1.926 (4)	O1–Cu–N3	92.4 (2)
Cu–N3	1.946 (5)	O3–Cu–N1	99.2 (2)
Cu–O3	1.948 (5)	O1–Cu–O3	87.5 (2)
C1–N1	1.307 (7)	O1–Cu–N1	171.8 (2)
C1–N2	1.337 (7)	O3–Cu–N3	175.7 (2)
N2–N3	1.370 (6)	N1–C1–N2	122.7 (5)
N3–C2	1.278 (7)	C1–N2–N3	122.7 (5)
C4–O1	1.301 (7)	N2–N3–C2	117.9 (5)
		C5–N4–C7	124.7 (5)

The chelate ligand is coordinated through phenoxide oxygen, azomethine and isothioamide nitrogen atoms in a monoanionic form, *i.e.*, in the same way as was found in $[\text{VO}_2(\text{PLITSC-H}) \cdot 2\text{H}_2\text{O}]^{13}$. The tridentate coordination results in the formation of one five-membered (isothiosemicarbazide) and one six-membered (pyridoxylidene) planar metallocycles. The whole ligand molecule, besides the oxygen atom of the hydroxymethyl group, shows a high degree of planarity, which can be associated with its extended system of conjugated double bonds. It is interesting to note that the metallocycles and the pyridoxal ring lie virtually in the same plane, characterized by dihedral angles of $2.31(9)^\circ$ between the five- and the six-membered metallocycles, and $2.9(1)^\circ$ between the five-membered metallocycle and the pyridoxal ring. These values are close to those found in complex $[\text{CuPLITSC}(\text{NO}_3)(\text{H}_2\text{O})]\text{NO}_3^{14}$ but significantly lower than those in the complexes $[\text{Cu}(\text{PLITSC})\text{Br}(\text{MeOH})]\text{Br}^{15}$ (5.2 and 4.7°) and $[\text{VO}_2(\text{PLITSC-H}) \cdot 2\text{H}_2\text{O}$ (12.0 and 7.8°),¹³ in which the deformation of the square-pyramidal environment is more pronounced.

As in all the hitherto structurally characterized complexes,^{12–15} PLITSC undergoes double spatial tautomerization, *i.e.*, migration of the phenolic hydrogen atom to pyridinic nitrogen atom, and migration of the hydrogen atom from the isothioamide nitrogen N1 to the neighboring nitrogen atom N2 of the hydrazine moiety. However, the nitrogen atom N2 under the given conditions is deprotonated, resulting in complex formation with the monoanionic form of PLITSC. This means that the pyridoxal moiety retains a zwitter-ionic form, which is confirmed by the value of the C6–N4–C8 angle ($124.7(5)^\circ$), which lies within the range characteristic for protonated pyridine rings.⁴

The fact that the structure of $[\text{Cu}(\text{PLITSC})\text{Br}(\text{MeOH})]\text{Br}$ (**3**) is known¹⁵ (CCDC-735806) enables the elucidation of the impact of the ligand deprotonation on the geometry of the formed complex, using comparative analysis. Namely, deprotonation of the hydrazine nitrogen atom leads to a slight shortening of the C1–N2 bond ($1.337(7)$ and $1.361(3)$ Å in **1** and **3**, respectively) and elongation of C1–N1 bond ($1.307(7)$ and $1.273(3)$ Å in **1** and **3**, respectively). This suggests that the electron pair is delocalized in the N2–C1–N1 fragment after the deprotonation, which is consistent with structural data reported for $[\text{VO}_2(\text{PLITSC-H}) \cdot 2\text{H}_2\text{O}]^{13}$. Moreover, deprotonation leads to angular changes in the isothiosemicarbazide moiety, expressed through shrinkages of the N1–C1–N2 and C1–N2–N3 angles from $122.7(5)^\circ$ in **1** to $118.3(2)^\circ$ in **3** and from $122.7(5)^\circ$ in **1** to $115.2(2)^\circ$ in **3**, respectively.

Besides ionic interaction, association of the complex molecules in the solid state is determined by the presence of multiple hydrogen bond donors and acceptors. All the potential hydrogen donors, except for N1, are involved in the formation of intermolecular hydrogen bonds, with geometric parameters summarized in Table III. These secondary interactions link molecules in sheets extend-

TABLE III. Geometry of the intermolecular interactions for **1**. Symmetry codes: (i) $x, y, z-1$; (ii) $x+\frac{1}{2}, -y+\frac{1}{2}, z+1$; (iii) $-x+\frac{1}{2}, y+\frac{1}{2}, z+\frac{1}{2}$; (iv) $x+\frac{1}{2}, -y+\frac{1}{2}, z$; (v) $x-\frac{1}{2}, -y+\frac{1}{2}, z$; α = dihedral angle between planes I and J; β = angle between $Cg(I)\rightarrow Cg(J)$ vector and normal to plane I; γ = angle between $Cg(I)\rightarrow Cg(J)$ vector and normal to plane J; rings: (1) = Cu,N1,C1,N2,N3; (2) = Cu,O1,C4,C3,C2,N3; (3) = N4,C5,C4,C3,C8,C7

Hydrogen bonds				
D-H···A	$d(D-H)/\text{\AA}$	$d(H\cdots A)/\text{\AA}$	$d(D\cdots A)/\text{\AA}$	$\angle(D-H\cdots A)/^\circ$
O3-H3B···O2 ⁱ	0.81	1.92	2.708 (6)	164.1
O3-H3A···O4	0.96	1.79	2.745 (6)	174.6
O2-H2···O4 ⁱⁱ	0.93	1.89	2.728 (7)	149.7
N4-H4···Br ⁱⁱⁱ	0.84	2.40	3.233 (4)	173.3
O4-H4A···Br	0.79	2.52	3.196 (4)	143.1
O4-H4B···N2 ⁱ	0.98	1.89	2.797 (6)	153.4
$\pi\cdots\pi$ Stacking interactions				
Cg(I)···Cg(J)	$d(Cg\cdots Cg)$	$\alpha/^\circ$	$\beta/^\circ$	$\gamma/^\circ$
Cg(1)···Cg(3) ^{iv}	3.480 (3)	2.3 (2)	9.3	7.2
Cg(1)···Cg(3) ^v	3.713 (3)	2.3 (2)	23.3	25.5
Cg(2)···Cg(2) ^v	3.504 (3)	3.4 (1)	14.4	12.2

ing in the bc plane, as depicted in Fig. 2, which are in turn connected through O2-H2···O4ⁱⁱ (symmetry code: (ii) $x+\frac{1}{2}, -y+\frac{1}{2}, z+1$) hydrogen bonds, as well as $\pi\cdots\pi$ stacking interactions (Table III), thus building a 3D supramolecular net-

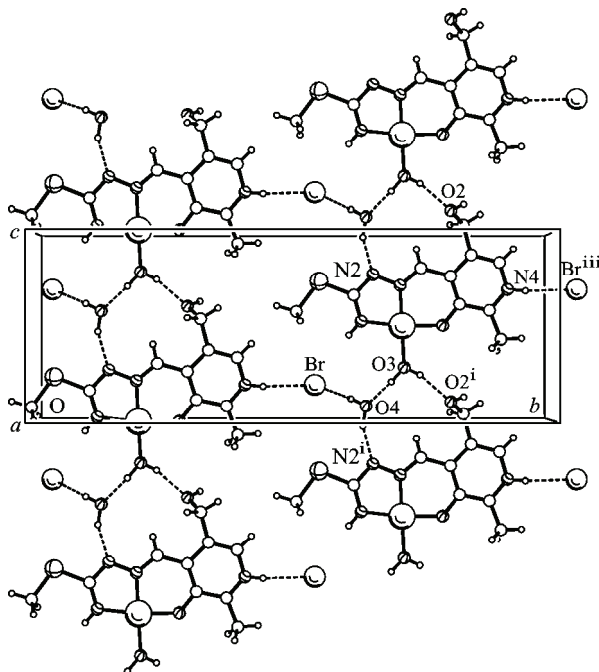


Fig. 2. Hydrogen bonded sheet in the bc plane of **1**. Symmetry codes are given in Table III.

work. Namely, zigzag puckered sheets are stacked in a way that the cations are lying parallel to each other at a *ca.* 3.4 Å distance. According to the literature,³¹, mutual orientation of the stacked six-membered metallocycles corresponds to *cross* conformation, based on Cu–Cg(2)–Cg(2)^V–Cu^V torsion angle of 86.8 (8)[°] (Cg(2) is centroid of the six membered metallocycle; symmetry code: (v) $x-\frac{1}{2}$, $-y+\frac{1}{2}$, z). The five membered metallocycle is involved in asymmetrical $\pi\cdots\pi$ interactions through the pyridine rings of two neighboring sheets.

Thermal analysis

To present the decomposition patterns of compounds **1–3**, their derivative thermogravimetric (DTG) curves are shown in Fig. 3. The thermal decomposition of **1** started with the evaporation of both crystal and coordinated water with an onset temperature of 99 °C and a maximum decomposition rate at 168 °C. Before complete water removal, the decomposition of the organic ligand starts. The amount of water found to the minimum in the DTG curve (at 197 °C, 8.3 %) agrees with the calculated one (8.33 %). While the decomposition of **1** is obviously different, according to their similar composition, the decomposition of complexes **2** and **3** is very similar (see Fig. 3). Namely, the difference is in one coordinated methanol in compound **3**. During storage at room temperature, the methanol is almost completely lost, so the better-separated peaks in the DTG curve of **3** refer to the different structure of the starting compound. MeOH seems to be trapped in the crystals of the freshly prepared compound and at \approx 150 °C, it evaporates in explosion-like steps. The decomposition in all three compounds is endothermic up to 250 °C, which at around 300 °C turns into an exothermic process. Under nitrogen, the decomposition is not complete at 700 °C.

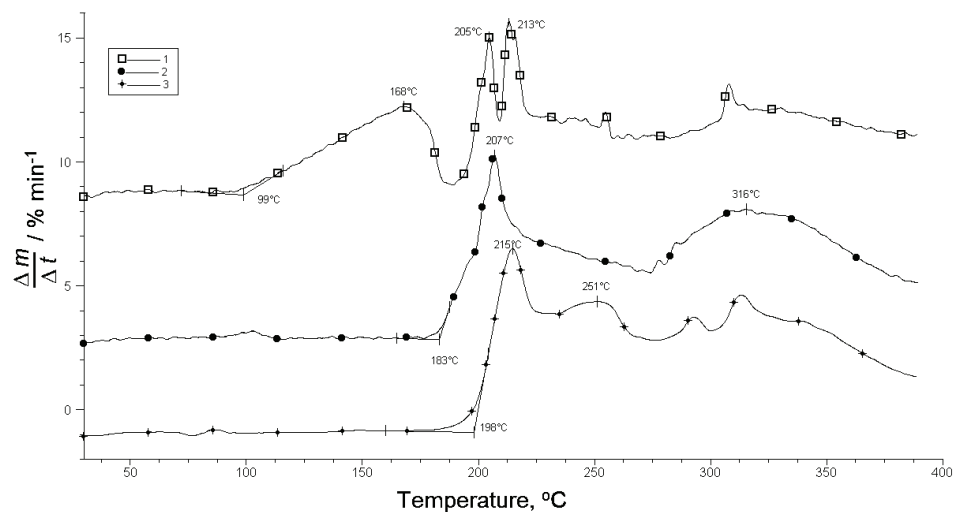


Fig. 3. DTG curves of complexes **1–3** in nitrogen atmosphere.

According to the thermal decomposition mechanism, it is very unlikely that the corresponding anhydrous compound of **1** could be prepared. Therefore, the thermal stability of **1** is rather low. Compounds **2** and **3** are practically stable up to about 180 °C, assuming that **3** had been left at room temperature until it had lost its MeOH. However, the thermal stability of complex **2** obtained by slow MeOH evaporation from **3**, due to different structure of the starting compound, is higher (see Fig. 3). Freshly prepared **3** is thermally stable up to around 150 °C.

SUPPLEMENTARY MATERIAL

Crystallographic data reported for the complex $[\text{Cu}(\text{PLITSC}-\text{H})(\text{H}_2\text{O})]\text{Br}\cdot\text{H}_2\text{O}$ (**1**) have been deposited with CCDC, No. CCDC-942238. Copies of the data can be obtained free of charge via www.ccdc.cam.ac.uk.

Acknowledgements. This work was supported by the Provincial Secretariat for Science and Technological Development of Vojvodina and the Ministry of Education, Science and Technological Development of the Republic of Serbia (Grant No. 172014).

ИЗВОД

КОМПЛЕКСИ ПРЕЛАЗНИХ МЕТАЛА СА ЛИГАНДИМА НА БАЗИ
ТИОСЕМИКАБАЗИДА. ДЕО 60. РЕАКЦИЈЕ БАКАР(II)-БРОМИДА СА
S-МЕТИЛИЗОТИОСЕМИКАБАЗОНОМ ПИРИДОКСАЛА (PLITSC). КРИСТАЛНА
СТРУКТУРА $[\text{Cu}(\text{PLITSC}-\text{H})\text{H}_2\text{O}]\text{Br}\cdot\text{H}_2\text{O}$

ВУКАДИН М. ЛЕОВАЦ¹, ЉИЉАНА С. ВОЈИНОВИЋ-ЈЕШИЋ¹, СОЊА А. ИВКОВИЋ², МАРКО В. РОДИЋ¹,
ЉИЉАНА С. ЈОВАНОВИЋ¹, BERTA HOLLÓ¹ и KATALIN MÉSZÁROS SZÉCSÉNYI¹

¹Природно-математички факултет, Универзитет у Новом Саду, Трг Д. Обрадовића 3,

21000 Нови Сад и ²Факултет заштите животне средине, Универзитет EDUCONS,

Б. Путничка бб, 21208 Сремска Каменица

Синтетисан је и структурно охарактерисан квадратно-планарни комплекс бакра(II) са S-метилизотиосемикарбазоном пиридоксала (PLITSC) формуле $[\text{Cu}(\text{PLITSC}-\text{H})\text{H}_2\text{O}]\text{Br}\cdot\text{H}_2\text{O}$ (**1**), који представља први комплекс Cu(II) са монаонјонском формом наведеног лиганда. Комплекс **1** као и два раније синтетисана комплекса $[\text{Cu}(\text{PLITSC})\text{Br}_2]$ (**2**) и $[\text{Cu}(\text{PLITSC})\text{Br}(\text{MeOH})]\text{Br}$ (**3**), охарактерисани су елементалном анализом, IR, UV-Vis спектрима, као и методама термичке анализе, кондуктометрије и магнетохемије.

(Примљено 22. јуна, ревидирано 20. августа 2013)

REFERENCES

1. J. S. Casas, M. D. Couce, J. Sordo, *Coord. Chem. Rev.* **256** (2012) 3036, and references therein
2. V. M. Leovac, V. S. Jevtović, Lj. S. Jovanović, G. A. Bogdanović, *J. Serb. Chem. Soc.* **70** (2005) 393, and references therein
3. M. Ferrari Belicchi, G. F. Gasparri, E. Leporati, C. Pelizzi, P. Tarasconi, G. Tosi, *J. Chem. Soc., Dalton Trans.* (1986) 2455
4. S. Floquet, M. Carmen Munoz, R. Guillot, E. Riviere, G. Blain, J.-A. Real, M.-L. Boillot, *Inorg. Chim. Acta* **362** (2009) 56
5. E. W. Yemeli Tido, C. Faulmann, R. Roswanda, A. Meetsma, P. J. van Koningsbruggen, *Dalton Trans.* **39** (2010) 1643

6. V. Vrdoljak, J. Pisk, B. Prugovečki, D. Matković-Čalogović, *Inorg. Chim. Acta* **362** (2009) 4059
7. V. M. Leovac, Lj. S. Jovanović, V. Divjaković, A. Pevec, I. Leban, T. Armbruster, *Polyhedron* **26** (2007) 49
8. M. Belicchi Ferrari, F. Bisceglie, C. Casoli, S. Durot, I. Morgenstern-Badarau, G. Pelosi, E. Pilotti, S. Pinelli, P. Tarasconi, *J. Med. Chem.* **48** (2005) 1671
9. V. S. Jevtović, Lj. S. Jovanović, V. M. Leovac, L. J. Bjelica, *J. Serb. Chem. Soc.* **68** (2003) 929
10. Lj. S. Jovanović, V. S. Jevtović, V. M. Leovac, L. J. Bjelica, *J. Serb. Chem. Soc.* **70** (2005) 187
11. V. Jevtović, D. Cvetković, D. Vidović, *J. Iran. Chem. Soc.* **8** (2011) 727
12. V. Jevtović, D. Vidović, *J. Chem. Crystallogr.* **40** (2010) 794
13. V. M. Leovac, V. Divjaković, M. D. Joksović, Lj. S. Jovanović, Lj. S. Vojinović-Ješić, V. I. Češljević, M. Mlinar, *J. Serb. Chem. Soc.* **75** (2010) 1063
14. V. M. Leovac, V. S. Jevtović, G. A. Bogdanović, *Acta Crystallogr., C* **58** (2002) 514
15. S. Ivković, V. Jevtović, *J. Eng. Process. Manag.* **2** (2010) 7
16. V. S. Jevtović, *Ph. D. Thesis*, Faculty of Science, University of Novi Sad, Novi Sad, 2002
17. CrysAlisPro Software system, version 1.171.35.19, Agilent Technologies UK Ltd., Oxford, 2011
18. A. Altomare, G. Cascarano, C. Giacovazzo, A. Gualandi, *J. Appl. Crystallogr.* **26** (1993) 343
19. G. M. Sheldrick, *Acta Crystallogr., A* **64** (2008) 112
20. C. B. Hübschle, G. M. Sheldrick, B. Dittrich, *J. Appl. Crystallogr.* **44** (2011) 1281
21. A. L. Spek, *Acta Crystallogr., D* **65** (2009) 148
22. L. J. Farrugia, *J. Appl. Crystallogr.* **30** (1997) 565
23. W. J. Geary, *Coord. Chem. Rev.* **7** (1971) 81
24. D. Poleti, Lj. Karanović, V. M. Leovac, V. S. Jevtović, *Acta Crystallogr., C* **59** (2003) 73
25. M. Belicchi Ferrari, G. G. Fava, C. Pelizzi, P. Tarasconi, G. Tosi, *J. Chem. Soc., Dalton Trans.* (1987) 227
26. E. W. Yemeli Tido, E. J. M. Vertelman, A. Meetsma, P. J. van Koningsbruggen, *Inorg. Chim. Acta* **360** (2007) 3896
27. M. R. Maurya, A. Kumar, M. Abid, A. Azam, *Inorg. Chim. Acta* **359** (2006) 2439
28. P. Kalaivani, R. Prabhakaran, E. Ramachandran, F. Dallemer, G. Paramaguru, R. Renganathan, P. Poornima, V. Vijaya Padma, K. Natarajan, *Dalton Trans.* **41** (2012) 2486
29. M. M. Lalović, V. M. Leovac, Lj. S. Vojinović-Ješić, M. V. Rodić, Lj. S. Jovanović, V. I. Češljević, *J. Serb. Chem. Soc.* **78** (2013) 1161
30. Lj. S. Jovanović, V. M. Leovac, unpublished results
31. D. N. Sredojević, Z. D. Tomić, S. D. Zarić, *Cryst. Growth Des.* **10** (2010) 3901.